Lanthanide Complexes of 2,6-Dihydroxybenzoic Acid: Synthesis, Crystal Structures and Luminescent Properties of $[n\mathrm{Bu_4N}]_2[\mathrm{Ln(2,6\text{-}dhb)_5(H_2O)_2}]$ (Ln = Sm and Tb)

Paula C. R. Soares-Santos,[a] Helena I. S. Nogueira,[a] Filipe A. Almeida Paz,[c] Rute A. Sá Ferreira,[b] Luís D. Carlos,[b] Jacek Klinowski,[c] and Tito Trindade*[a]

Keywords: Lanthanides / O ligands / Luminescence / Triboluminescence

Lanthanide complexes of 2,6-dihydroxybenzoic acid (2,6-Hdhb), namely $[n\mathrm{Bu_4N}]_2[\mathrm{Ln(2,6\text{-}dhb)_5(H_2O)_2}]$ [Ln = Sm (**1**) and Tb (**2**)], were synthesized and their crystal structures determined by single-crystal X-ray diffraction studies. The 2,6-$\mathrm{dhb^-}$ ligand coordinates to the lanthanide cations through the carboxylate group in a monodentate or bidentate chelating coordination mode. The compounds were further characterised using IR, Raman, ^{1}H and ^{13}C NMR spectroscopy and elemental analysis. Photoluminescence measurements were performed on both compounds. In particular, the terbium complex **2** shows intense photoluminescence both in the solid state and in ethanolic solution. Compound **2** also exhibits triboluminescence.

Introduction

Interest in the photophysical properties of lanthanide ion complexes has grown considerably in the last few years[1−3] since Lehn proposed that such complexes could be used as light conversion molecular device units (LCMDs).[4] Appropriate organic ligands can act as light collectors (antenna) and transfer absorbed energy to the coordinated lanthanide ion (emitter). These highly luminescent lanthanide complexes can act as functional units for the creation of luminescent devices on the nanoscale or molecular scale. We have been interested in the synthesis and characterisation of such complexes and in particular, lanthanide compounds containing aromatic ambidentate ligands in the first coordination shell.[5]

Complexes of Y^{3+}, La^{3+}, Pr^{3+}, Nd^{3+}, Sm^{3+} and Gd^{3+} with 2,6-dihydroxybenzoic acid (2,6-Hdhb) have been reported, along with their IR and UV/Vis spectra in ethanolic solutions, but their molecular formulae were not determined.[6] Brzyska et al. investigated the IR spectra and the thermal behaviour of 2,6-Hdhb complexes for a series of lanthanides including those of Y^{3+}, the series La^{3+} to Eu^{3+}[7] and Gd^{3+} to Lu^{3+},[8] with general formulae being proposed as $[\mathrm{Ln(C_7H_5O_4)_3}]\cdot n\mathrm{H_2O}$, where $n = 4$ for Ln = La^{3+} to Sm^{3+}, $n = 6$ for Eu^{3+}; $[\mathrm{Ln(C_7H_5O_4)_3(H_2O)_4}]\cdot 2\mathrm{H_2O}$ for Ln = Y^{3+} and Gd^{3+} to Lu^{3+}.[8] Glowiak et al. reported the crystal structures of the Tb^{3+} and Ho^{3+} complexes of 2,6-Hdhb,[9] confirming their molecular formula. 2,6-Hdhb complexes of the d-block metals have also been reported, namely those of Mo^{VI}, Os^{VI},[10] Re^{V},[10,11] Cu^{II} [12] and Ag^{I}.[13]

Here we report the synthesis and structural characterisation of new Sm^{3+} and Tb^{3+} complexes of 2,6-Hdhb. The 2,6-Hdhb ligand shows different coordination modes, either using both the carboxylate group and an adjacent hydroxy group in a salicylato-type chelate,[11] or utilising only the carboxylate group in a monodentate[12] or bidentate fashion.[9,14] The crystal structures of the complexes $[n\mathrm{Bu_4N}]_2[\mathrm{Ln(2,6\text{-}dhb)_5(H_2O)_2}]$ [Ln = Sm (**1**) and Tb (**2**)], were determined by single-crystal X-ray diffraction studies.

In complexes **1** and **2** the 2,6-$\mathrm{dhb^-}$ ligand coordinates both in a monodentate or chelating bidentate manner which is in contrast to that seen in similar compounds reported in the literature.[9] The photoluminescent behaviour of the complexes was investigated and the photophysical properties of the Tb^{3+} complex **2** were studied both in the solid state and in ethanolic solution. It was found that when compound **2** was subjected to mechanical force, luminescence was observed. This phenomenon is known as triboluminescence and the corresponding spectrum for compound **2** is presented and discussed. The compound $[\mathrm{Tb(2,6\text{-}dhb)_3(H_2O)_4}]\cdot 2\mathrm{H_2O}$ (**3**), previously reported by

[a] Department of Chemistry, University of Aveiro, CICECO, 3810-193 Aveiro, Portugal
E-mail: ttrindade@dq.ua.pt
[b] Department of Physics, University of Aveiro, CICECO, 3810-193 Aveiro, Portugal
E-mail: lcarlos@fis.ua.pt
[c] Department of Chemistry, University of Cambridge, Lensfield Road, Cambridge CB2 1EW, U.K.
E-mail: jk18@cam.ac.uk

Brzyska et al.,[8] was also synthesized by us in order to perform comparative photoluminescence studies with our new compounds.

Results and Discussion

Crystal Structures of $[n\mathrm{Bu_4N}]_2[\mathrm{Ln(2,6\text{-}dhb)_5(H_2O)_2}]$ Complexes

Single-crystal X-ray diffraction studies revealed similar crystal structures for the Sm^{3+} and Tb^{3+} complexes, which crystallise in the chiral and non-centrosymmetric $P2_1$ space group. The molecular formulae were calculated as $[n\mathrm{Bu_4N}]_2[\mathrm{Ln(2,6\text{-}dhb)_5(H_2O)_2}]$ [where Ln = Sm^{3+} (**1**) and Tb^{3+} (**2**)] (Table 1). Phase purity and homogeneity of the bulk samples were confirmed by elemental analyses and X-ray powder diffraction experiments. The crystal structures contain only one crystallographically unique metal centre coordinated to five 2,6-dhb$^-$ organic ligands and two water molecules, in a geometry which is best described as a distorted tricapped trigonal prism (Figures 1 and 2, Tables 2 and 3). The $[\mathrm{Ln(2,6\text{-}dhb)_5(H_2O)_2}]^{2-}$ complex anions (Ln = Sm^{3+} and Tb^{3+}) are chiral and the average Ln−O distance for the coordinated solvent molecules is 2.45 and 2.41 Å (for compounds **1** and **2**, respectively), in good agreement with reported results for other Ln complexes.[15] 2,6-dhb$^-$ appears as an *exo*-monodenate ligand forming two coordinative η^3-*syn*,*syn*-chelates and three *syn*-unidentate bonds to the lanthanide centres. All the carboxylate groups maintain the equivalence of the C−O bonds, with the distances being in the 1.26−1.28 Å range (Table 2). This is particularly unexpected for the unidentate groups, and can be explained by the presence of strong hydrogen bonds with the water molecules (Table 4).[16] The average O−C−O angles for the carboxylate groups (121.5 and 121.4° for **1** and **2**, respectively) are also close to the expected values.[16] An interesting feature of the crystal is the medium-intensity hydrogen bond between the O2 water molecule and the O14 hydroxy group of the neighbouring $[\mathrm{Ln(2,6\text{-}dhb)_5(H_2O)_2}]^{2-}$ complex ($O2\cdots O14^{i} \approx 2.9$ Å; symmetry code i: $x-1, y, z$), leading to the formation of a hydrogen-bonded metal chain which runs along the *a* direction of the unit cell (Figures 2 and 3, Table 4). Each hydroxy group of the 2,6-dhb$^-$ ligands is also involved in strong hydrogen bonding with the nearest oxygen atoms (Table 4).

Vibrational and NMR Spectra

Selected IR and Raman spectroscopic data for the free ligand 2,6-Hdhb, the tetrabutylammonium salt of the 2,6-dhb$^-$ ligand, $[n\mathrm{Bu_4N}]$[2,6-dhb], and the lanthanide complexes are shown in Table 5. Tentative assignments are based on those found in the literature for other 2,6-Hdhb complexes.[10,11] The IR spectra of the 2,6-dhb$^-$ tetrabutylammonium salt and of the lanthanide complexes both exhibit a broad band with a maximum in the region 3453−3419 cm^{-1} which can be assigned to the phenolic ν(O−H) stretch (3478 cm^{-1} in the free ligand) and to the coordinated water molecules. The corresponding δ(OH) bend is observed at 1351 cm^{-1} in the ligand, at 1345 cm^{-1} in the 2,6-dhb$^-$ tetrabutylammonium salt and at 1355 cm^{-1} in the complexes. The IR and Raman spectra of the free ligand both show a very strong band which may be assigned to the ν(C=O) at 1681 and 1674 cm^{-1}, respectively. In the

Table 1. Crystal data and structure refinement information for **1** and **2**

	1	**2**
Empirical formula	$C_{67}H_{101}N_2O_{22}Sm$	$C_{67}H_{101}N_2O_{22}Tb$
Formula mass	1436.85	1445.42
Crystal system	monoclinic	monoclinic
Space group	$P2_1$	$P2_1$
a [Å]	11.089(2)	11.061(2)
b [Å]	23.395(5)	23.371(5)
c [Å]	14.632(3)	14.598(3)
β [°]	109.87(3)	109.72(3)
Volume [Å^3]	3569.8(12)	3552.6(12)
Z	2	2
$D_{calcd.}$ [g cm^{-3}]	1.337	1.351
μ(Mo-K_α) [mm^{-1}]	0.896	1.069
Crystal size [mm]	0.23 × 0.16 × 0.12	0.16 × 0.10 × 0.05
Crystal type	colourless blocks	orange blocks
θ range [°]	3.68−27.48	3.79−27.41
Index ranges	$-14 \le h \le 14$ $-30 \le k \le 28$ $-18 \le l \le 19$	$-14 \le h \le 13$ $-30 \le k \le 26$ $-18 \le l \le 18$
Reflections collected	26761	32607
Independent reflections	14390 (R_{int} = 0.0336)	13984 (R_{int} = 0.0572)
Absolute structure parameter	−0.017(7)	−0.021(7)
Final *R* indices [$I > 2\sigma(I)$]	$R1$ = 0.0340, $wR2$ = 0.0880	$R1$ = 0.0411, $wR2$ = 0.0828
Final *R* indices (all data)	$R1$ = 0.0388, $wR2$ = 0.0936	$R1$ = 0.0584, $wR2$ = 0.0889
Largest diff. peak and hole [e Å^{-3}]	0.917 and −0.840	0.913 and −0.677

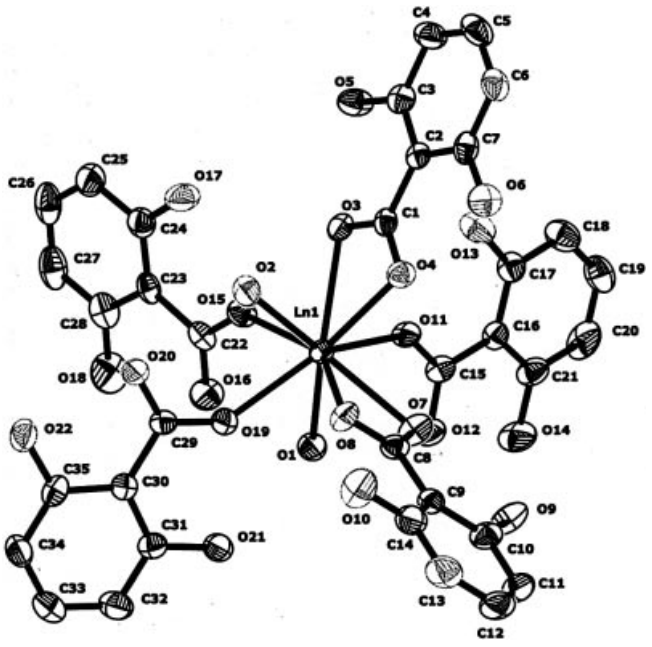

Figure 1. Chiral complex anion, $[Ln(2,6\text{-dhb})_5(H_2O)_2]^{2-}$, present in the crystal structures of **1** and **2**, showing the distorted tricapped trigonal-prismatic $\{LnO_9\}$ coordination environment for the crystallographically unique metal centres (Ln = Sm^{3+} or Tb^{3+}); hydrogen atoms are omitted for clarity; thermal displacement ellipsoids are drawn at the 50% probability level

Table 2. Selected bond lengths [Å] for **1** and **2**

	1	**2**
Ln1−O1	2.464(3)	2.419(3)
Ln1−O2	2.446(3)	2.407(3)
Ln1−O3	2.531(4)	2.506(4)
Ln1−O4	2.526(3)	2.486(3)
Ln1−O7	2.473(3)	2.448(3)
Ln1−O8	2.552(4)	2.515(5)
Ln1−O11	2.455(3)	2.422(3)
Ln1−O15	2.377(3)	2.326(3)
Ln1−O19	2.433(3)	2.401(3)
C1−O3	1.265(5)	1.287(5)
C1−O4	1.271(5)	1.271(6)
C8−O7	1.279(5)	1.276(6)
C8−O8	1.267(5)	1.269(6)
C15−O11	1.280(4)	1.271(5)
C15−O12	1.272(5)	1.280(6)
C22−O15	1.282(5)	1.283(5)
C22−O16	1.258(5)	1.251(6)
C29−O19	1.270(5)	1.267(5)
C29−O20	1.265(5)	1.263(5)

Table 3. Selected bond angles [°] for **1** and **2**

	1	**2**
O1−Ln1−O2	135.60(10)	136.17(11)
O1−Ln1−O3	131.52(11)	131.88(13)
O1−Ln1−O4	145.48(10)	145.33(10)
O1−Ln1−O7	70.86(10)	71.00(12)
O1−Ln1−O8	98.33(12)	97.98(14)
O1−Ln1−O11	73.11(10)	73.60(11)
O1−Ln1−O15	77.32(10)	77.78(12)
O1−Ln1−O19	66.57(10)	66.60(11)
O2−Ln1−O3	73.47(12)	73.13(14)
O2−Ln1−O4	78.53(10)	77.87(11)
O2−Ln1−O7	132.45(11)	131.99(13)
O2−Ln1−O8	82.01(12)	81.28(15)
O2−Ln1−O11	142.95(11)	142.37(13)
O2−Ln1−O15	79.90(11)	80.33(13)
O2−Ln1−O19	71.47(11)	71.62(12)
O11−Ln1−O3	69.50(10)	69.25(12)
O11−Ln1−O4	79.40(9)	79.73(11)
O11−Ln1−O7	71.98(10)	71.99(12)
O11−Ln1−O8	122.04(11)	122.83(12)
O11−Ln1−O15	87.29(11)	87.15(12)
O11−Ln1−O19	138.98(9)	139.26(11)
O15−Ln1−O3	71.26(10)	70.98(12)
O15−Ln1−O4	122.28(9)	123.02(11)
O15−Ln1−O7	145.81(10)	146.16(12)
O15−Ln1−O8	148.20(11)	147.67(13)
O15−Ln1−O19	77.07(11)	76.55(12)
O19−Ln1−O3	135.97(10)	135.17(12)
O19−Ln1−O4	140.68(9)	140.17(11)
O19−Ln1−O7	100.75(11)	101.93(13)
O19−Ln1−O8	72.45(11)	72.50(13)

spectra of the complexes, the assymetric $\nu_{as}(CO_2)$ is shifted to a higher wavenumber by up to 11 cm^{-1} upon coordination, when compared with the tetrabutylammonium salt of the 2,6-dhb^- ligand (1633 cm^{-1}). The symmetric mode $\nu_s(CO_2)$ also shows shifts to a higher wavenumber upon coordination (1292 cm^{-1} in the complexes) when compared with the tetrabutylammonium salt of the ligand (1286 cm^{-1}). The band at 1241 cm^{-1} in the spectrum of the tetrabutylammonium salt of the ligand, assigned to the $\nu(C-O)_h$ stretch (at 1236 cm^{-1} in the free ligand) of the phenolic groups, shifts to 1228 cm^{-1} on coordination, possibly due to hydrogen bonding.

^1H and ^{13}C NMR spectroscopic data for the free ligand and its lanthanide complexes in deuterated dimethyl sulfoxide solution are given in Table 6 (see Scheme 1 for labelling and Table 6 for tentative assignments). In the ^1H NMR spectra, the line arising from H^3 and H^5 appears as a doublet, and the line arising from H^4 as a triplet, with relative intensities of 2:1, respectively, either in the free ligand or in the complexes. The resonances of these protons shift to higher field on coordination. The resonances due to the protons of the counterion can also be observed in the spectra of the complexes. The resonances of the aromatic protons in **2** show higher shifts when compared with the values obtained for **1**, which may be induced by the Tb^{III} ion. In the spectra of **1** and **2** we can also observe resonances due to the phenolic protons as a broad signal (at δ = 14.5 and 14.0 ppm), with relative intensities of 2:1 when compared with the line assigned to H^4.

^{13}C NMR spectroscopy shows the resonances of all the carbon atoms, both of the ligand and the counterion. The most relevant shifts are observed in the signal of the carboxylate atom C^7, which shifts to lower-field on coordination, showing that the ligand is bound to the lanthanide atom through the carboxylate oxygen atoms.

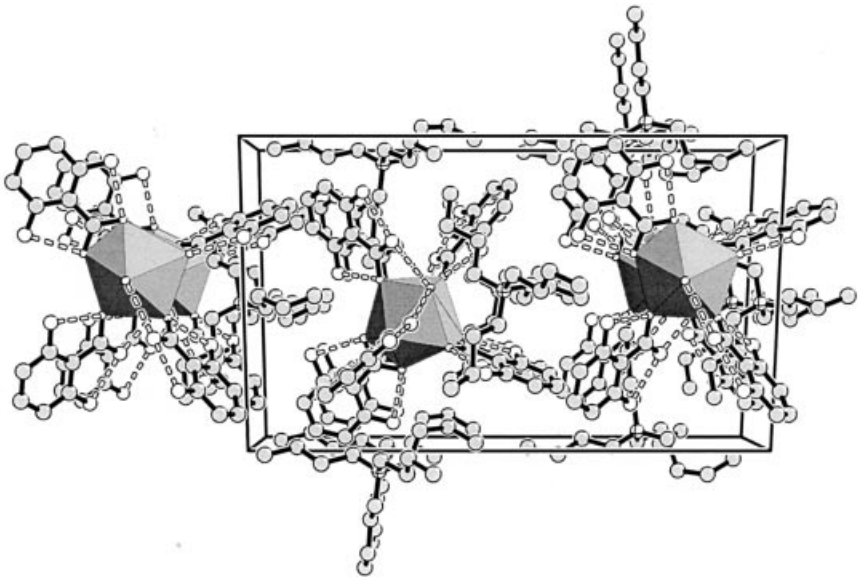

Figure 2. Perspective along the *a* axis of $[n\mathrm{Bu_4N}]_2[\mathrm{Ln(2,6\text{-}dhb)_5(H_2O)_2}]$; lanthanide centres are represented as polyhedra and hydrogen bonds (see Table 4) as white-filled dashed lines

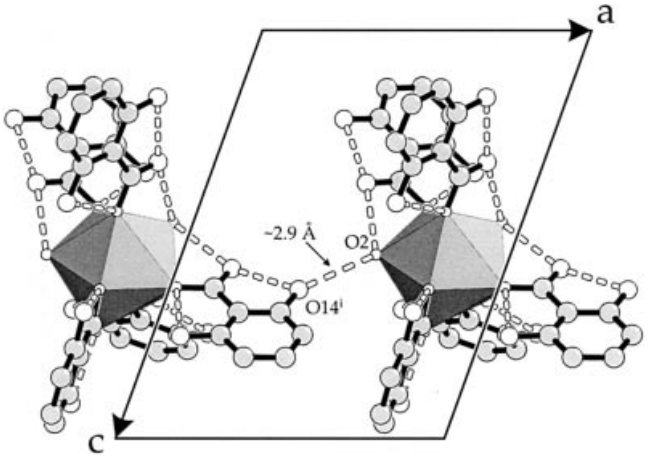

Figure 3. View along the *b* axis showing the hydrogen bond linking neighbouring $[\mathrm{Ln(2,6\text{-}dhb)_5(H_2O)_2}]^{2-}$ complexes; lanthanide centres are represented as polyhedra and hydrogen bonds (see Table 4) as dashed lines; symmetry code i: $x - 1, y, z$

Table 4. Distances [Å] and angles [°] between donors (D) and acceptors (A) for the D−H···A hydrogen bonds present in the crystal structures of **1** and **2**; symmetry code i: $x - 1, y, z$

	1		**2**	
D···A	*d*(D···A)	<(D−H···A)	*d*(D···A)	<(D−H···A)
O1···O12	2.644(4)	159(5)	2.642(5)	161(5)
O1···O16	2.725(5)	157(5)	2.713(5)	165(5)
O2···O20	2.726(4)	155(5)	2.712(5)	159(5)
O2···O14^{i}	2.907(4)	155(4)	2.954(5)	162(4)
O5···O3	2.553(5)	147(5)	2.553(6)	148(5)
O6···O4	2.591(4)	147(5)	2.594(4)	148(5)
O9···O7	2.552(5)	148(5)	2.540(5)	148(5)
O10···O8	2.573(5)	146(5)	2.561(7)	148(5)
O13···O11	2.572(4)	146(5)	2.569(5)	146(5)
O14···O12	2.510(4)	149(5)	2.517(5)	149(5)
O17···O15	2.547(4)	147(5)	2.563(5)	146(5)
O18···O16	2.512(5)	148(5)	2.522(5)	148(5)
O21···O19	2.584(4)	146(5)	2.594(5)	146(5)
O22···O20	2.528(4)	148(5)	2.534(5)	148(5)

Luminescence Spectra

Figures 4 and 5 show the room-temp. photoluminescence (PL) features of compounds **1**, **2** and **3**, excited at 350, 344 and 342 nm, respectively. The emission spectrum of the Sm^{3+} complex (Figure 4) is composed of a large broad band between 380 and 500 nm and a series of straight lines assigned to intra-4f^5 transitions between the $^4G(4)_{5/2}$ and the $^6H_{5/2,7/2,9/2,11/2}$ levels. Apart from a red shift (2000 cm^{-1}), the large broad band was already observed in the emission spectrum of 2,6-Hdhb, as shown in the inset of Figure 4. In the emission spectra of the Tb^{3+} compounds **2** and **3** only the intra-4f^8 lines, corresponding to transitions between the $^5D_4$ and $^7F_{6-0}$ levels, could be detected (Figure 5). The fact that the ligand's broad band could not be observed, clearly indicates a more efficient energy transfer between the Tb^{3+} ions and the 2,6-dhb ligand than that involving the Sm^{3+} cations.

The Tb^{3+} emission of compound **2** was compared with that of compound **3** and with the emission arising from compound **2** in a 1.4 mM alcoholic solution (Figure 5). All the spectra display the typical Tb^{3+} lines resulting from $^5D_4 \rightarrow {}^7F_{6-0}$ transitions. The emission lines of the Tb^{3+} alcoholic solution are almost identical to the ones observed for the powdered compound **2** in terms of energy and full width at half maximum. However, the Tb^{3+} transitions in compound **3** are more structured, providing evidence for a higher number of Stark components. In order to evaluate accurately the PL differences between the two Tb^{3+} solid samples, the respective emission spectra were measured at 10 K (Figure 6, A and B).

Table 5. Analytical and vibrational data for 2,6-dihydroxybenzoic acid and the Sm^{III} and Tb^{III} complexes

Compound	Analysis[a] C	N	H	Ln	Vibrational spectra[b] [cm^{-1}] $\nu_{as}(CO_2)$	$\delta(OH)$	$\nu_s(CO_2)$	$\nu(C-O)_h$
2,6-dihydroxybenzoic acid					1681 vs	1351 m	1294 m	1236 s
					1674(7)	1353(1)	1308(5)	1226(4)
[nBu$_4$N][2,6-dhb]					1633 vs	1345 m	1286 s	1241 vs
					1628(1)	1356(1)	1285(2)	1236(1)
[nBu$_4$N]$_2$[Sm(2,6-dhb)$_5$(H$_2$O)$_2$] (**1**)	55.08	1.96	7.14	10.53	1643 vs	1355 s	1292 s	1228 vs
	(56.00)	(1.95)	(7.09)	(10.45)	1649(2)	1355(1)	1298(10)	1231(1)
[nBu$_4$N]$_2$[Tb(2,6-dhb)$_5$(H$_2$O)$_2$] (**2**)	55.20	1.98	7.06	10.12	1644 vs	1355 s	1292 s	1228 vs
	(55.67)	(1.94)	(7.04)	(11.01)	1649(2)	1355(1)	1292(10)	1231(1)

[a] Calcd. values in parentheses. [b] Infrared and Raman (in italics) data; vs − very strong, s − strong, m − medium.

Table 6. ^1H and $^{13}C\{^1H\}$ NMR spectroscopic data for 2,6-dihydroxybenzoic acid and the Sm^{III} and Tb^{III} complexes

	Chemical shift [ppm][a] H^3	H^4	H^5	C^1	C^2	C^3	C^4	C^5	C^6	C^7
2,6-Dihydroxybenzoic acid	6.32 d	7.20 t	6.32 d	102.6	160.7	106.7	134.3	106.7	160.7	172.6
[nBu$_4$N]$_2$[Sm(2,6-dhb)$_5$(H$_2$O)$_2$] (**1**)	6.05 d	6.95 t	6.05 d	104.5	162.4	105.0	131.9	105.0	162.4	175.5
[nBu$_4$N]$_2$[Tb(2,6-dhb)$_5$(H$_2$O)$_2$] (**2**)	5.82 d	6.77 t	5.82 d	95.9	161.9	104.3	131.8	104.3	161.9	176.9

[a] Spectra in DMSO solution; d − doublet, t − triplet.

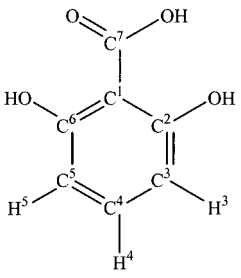

Scheme 1

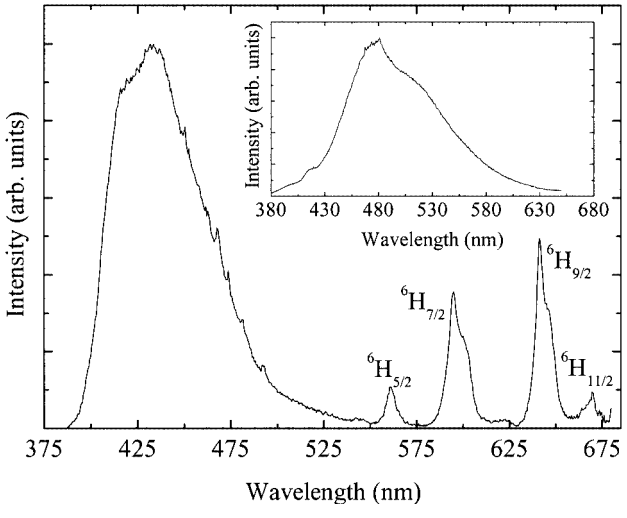

Figure 4. Room-temp. PL spectrum of [nBu$_4$N]$_2$[Sm(2,6-dhb)$_5$(H$_2$O)$_2$]; the inset shows the room-temp. PL spectrum of the 2,6-Hdhb ligand excited at 341 nm

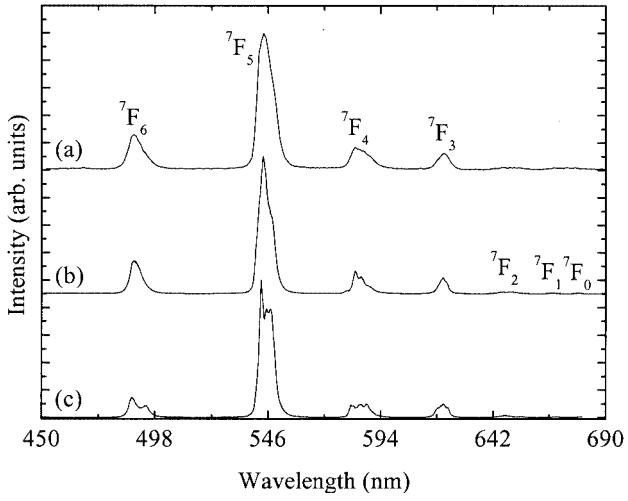

Figure 5. Room-temp. PL spectra of (a) 1.4 mM ethanolic solution of **2**, (b) compound **2** and (c) compound **3**

The most evident change with the decrease in temperature is related to the increase in the number of identified Stark components. For instance, in the most intense transition namely $^5D_4 \rightarrow {}^7F_5$, we can clearly distinguish 22 Stark components in both samples (Figure 6). Focusing our attention in the region of the $^5D_4 \rightarrow {}^7F_0$ transition, at least two lines, separated by 36 cm^{-1}, are undoubtedly discernable in the emission spectrum of **3**. For compound **2** the $^5D_4 \rightarrow {}^7F_0$ transition has a large value of 46 cm^{-1} for its full width at half maximum, suggesting the presence of more than one emission line. Since the Tb^{3+} ions lie in the same average local symmetry site (in agreement with the XRD data) and the $^7F_0$ is a non-degenerated level, the de-

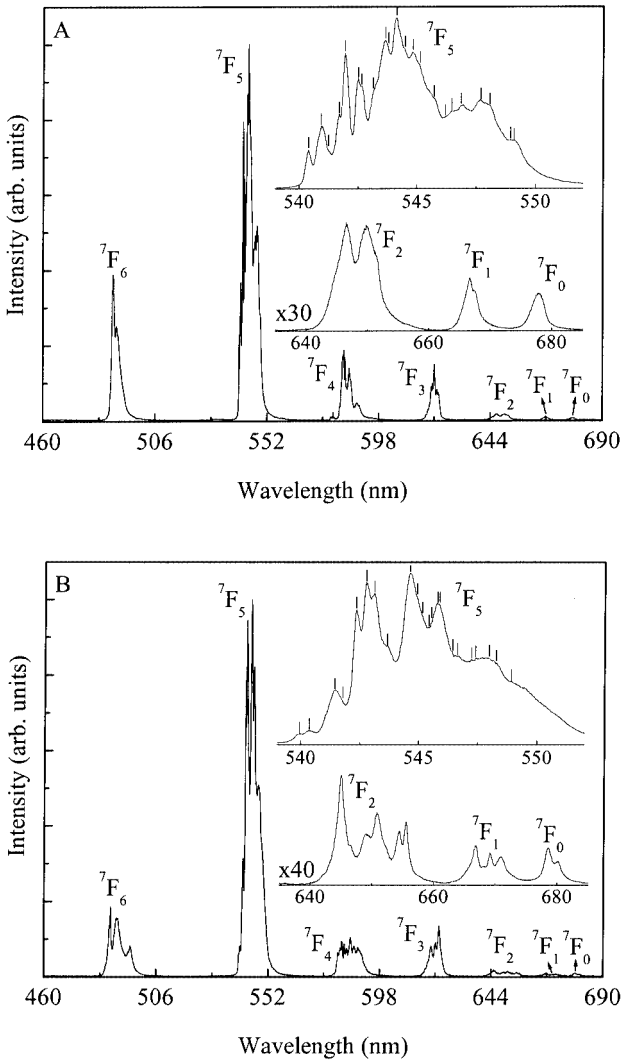

Figure 6. PL spectra, recorded at 10 K under 344 nm excitation wavelength of compound **2** (A) and compound **3** (B)

tection of more than one component in the $^5D_4 \rightarrow {}^7F_0$ region points to the thermal population of the upper $^5D_4$ levels. Even at 10 K, the emission from such levels, usually termed as hot lines, is not quenched making the emission spectra quite intricate.[17] These hot lines are responsible for the higher number of components perceived in the remaining transitions (Figure 6, A and B) and, thus, the observed local-field splitting of the $^5D_4 \rightarrow {}^7F_{1-6}$ transitions are in agreement with the point site symmetry group identified by XRD.

The differences observed between compounds **2** and **3** clearly indicate that the synthetic procedure results in different local coordination sites for the Tb^{3+} ions. On the contrary, dissolving the former compound in ethanol did not produce significant changes in the PL properties of the Tb^{3+}. This result suggests that the lanthanide ions are well shielded by the ligands from the incorporation of solvent molecules in the first coordination sphere which would contribute to the quenching of the emission intensity.

Figure 7 shows the room-temp. excitation (PLE) spectrum of the Sm^{3+} complex monitored around the cation's more intense line at 641 nm. The spectrum displays a large broad band between 250 and 420 nm, centred around 330 nm, and a series of sharp lines characteristic of the Sm^{3+} energy levels.

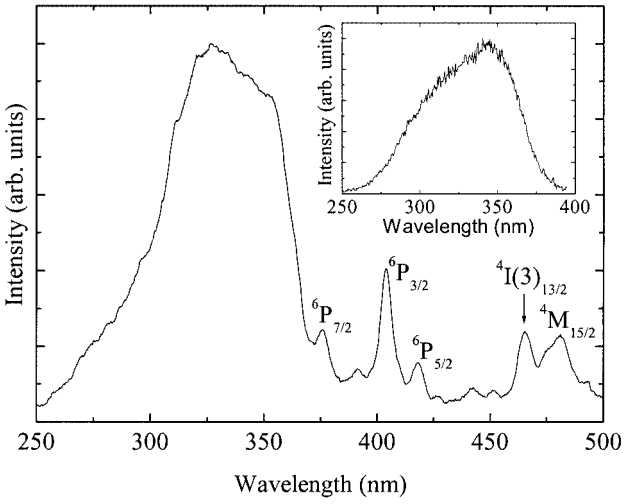

Figure 7. Room-temp. PLE spectrum of compound **1**; the inset shows the room-temp. PLE spectrum of the 2,6-Hdhb ligand detected around 480 nm

Figure 8 shows the PLE spectra of compounds **2** and **3** and of a 1.4 mM alcoholic solution of **2**. All the spectra exhibit a large broad band in the same spectral region of that observed in the PLE spectrum of the Sm^{3+}-based complex. The excited levels were only detected in the PLE spectrum of the Tb^{3+} solution. The large broad band is centred around 344, 342 and 327 nm, for **2**, **3** and the alcoholic solution, respectively. This band may be related to the ligand's excited states, since the PLE spectrum of the 2,6-

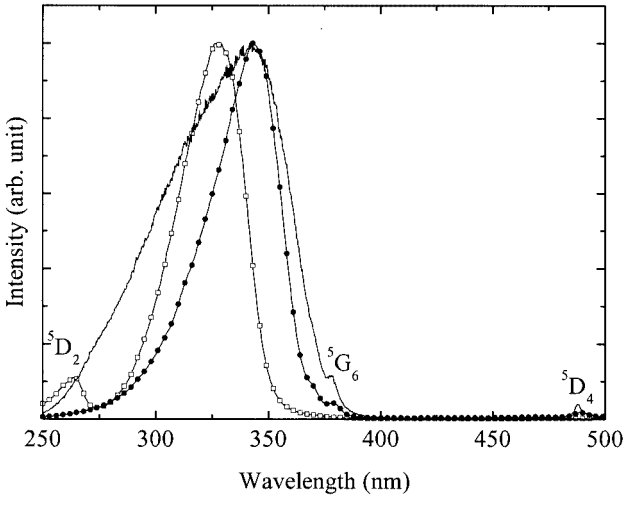

Figure 8. Room-temp. PLE spectra of compound **2** (solid line with solid circles), compound **3** (solid line) and a 1.4 mM ethanolic solution of **2** (solid line with open squares)

Hdhb ligand is characterized by a similar large broad band with peaks around 341 nm (inset of Figure 7).

The lifetimes of the $^5D_4$ Tb^{3+} excited levels were measured at room temperature under the excitation wavelength that maximizes their luminescent intensity for the two powdered complexes and for the ethanolic solution. The monitoring wavelength was set around the more intense emission line (544 nm). The lifetime of the $^4G(4)_{5/2}$ Sm^{3+} excited level could not be recorded since it lies in a time scale below our lower experimental detection limit (10^{-5} s). Figure 9 depicts the experimental data in a logarithmic scale for the three Tb^{3+}-based samples. All the data were well fitted by a single exponential function, confirming that all lanthanide ions occupy the same average local environment within each complex.

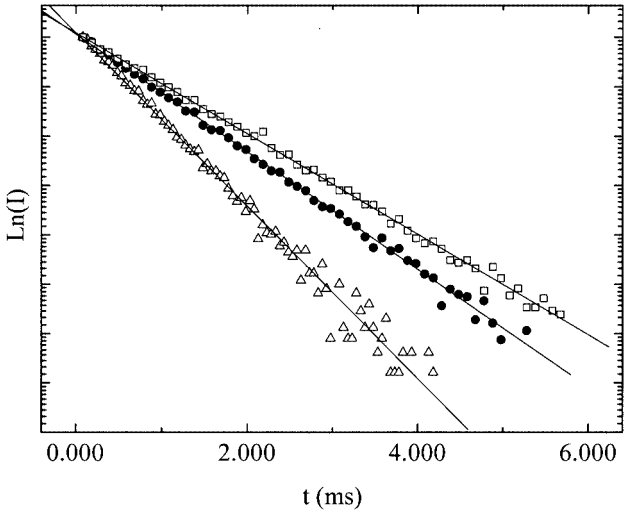

Figure 9. Room-temp. decay curves for compound **2** (solid circles), compound **3** (open triangles) and a 1.4 mM ethanolic solution of **2** (open squares); the solid lines represent the data best fits, assuming a single-exponential function ($r > 0.99$)

The $^5D_4$ lifetimes of **2** and the corresponding 1.4 mM ethanolic solution are 0.876 ±0.012 and 0.983 ±0.007 ms, respectively. Both values are similar, confirming the previous suggestion that solvation did not induce significant changes on the Tb^{3+} local environment, meaning that the ligands are efficiently shielding the lanthanide ions. The $^5D_4$ lifetime for **3** is smaller than the previous two values, being 0.562 ±0.001 ms. This decrease indicates that non-radiative pathways are more important in the latter complex. In fact, if we recall the local Tb^{3+} structure in both complexes, the lanthanide's first coordination sphere in **2** and **3** differs in the number of water molecules by two and four, respectively. It is well known that the presence of OH oscillators in the lanthanide first coordination sphere provides an efficient non-radiative path, so we can suggest that the observed decrease in the lifetime of the $^5D_4$ level is mainly related to an increase in non-raditive transitions due to the increase in the number of OH oscillators in the Tb^{3+} first coordination shell, which is in perfect agreement with the proposed structural results.

When ground by hand in daylight, single crystals of **2** exhibit green luminescence detectable by the naked-eye (Figure 10). The spectrum exactly matches that observed by excitation using UV light, indicating that triboluminescence (TL) involves the same Tb^{3+} excited-state deactivation as that observed in PL. The mechanisms behind TL are not well understood and predictions of this behaviour for a specific compound cannot be made. While TL behaviour of some compounds has been attributed to the piezoelectric properties of non-centrosymmetric crystals, many TL centrosymmetric crystals have also been reported.[18] Compound **2** is a non-centrosymmetric ionic complex and it has been suggested[18,19] that TL arises from charge separation by partial fracture along oppositely charged planes. Further work is under way to clarify the nature of the TL mechanism in this compound.

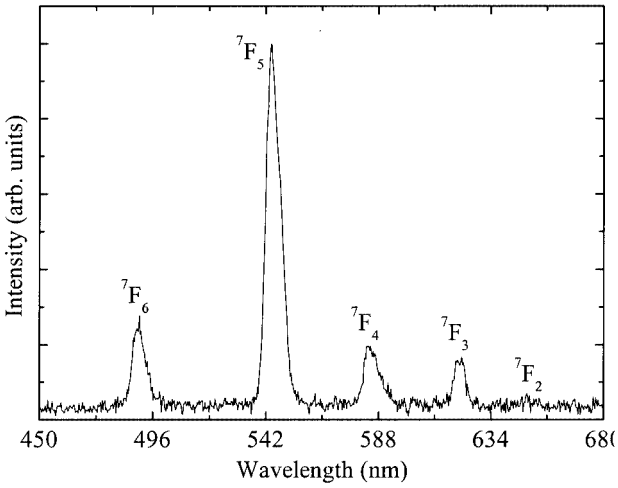

Figure 10. Room-temp. TL spectrum of compound **2**

Conclusion

New samarium and terbium complexes of 2,6-dihydroxybenzoic acid, each containing five 2,6-dhb$^-$ ligands coordinated to the metal centres and two tetrabutylammonium cations, have been synthesized and structurally characterized. The X-ray crystal structures show the carboxylate groups acting both as monodentate or bidentate chelating ligands; two water molecules complete the first coordination shell with a coordination number of nine. The luminescent properties of the Tb^{3+} complex with the 2,6-dhb$^-$ ligand are described here for the first time. The Tb^{3+} complex shows very high luminescence, even in an ethanolic solution. These particular luminescent properties may be explored in order to develop solution methods based on new luminescent materials in which this molecular unit could act as the active centre. Given its triboluminescent behaviour, the terbium compound is a potential candidate for the development of optical sensors.

Experimental Section

General: All chemicals were supplied by Aldrich and used without further purification. The terbium complex [Tb(2,6-dhb)$_3$(H$_2$O)$_4$]·2H$_2$O (**3**) was synthesized as described by Brzyska et al.[8]

Preparation of [*n*Bu$_4$N]$_2$[Ln(2,6-dhb)$_5$(H$_2$O)$_2$] [Ln = Sm (1) and Tb (2)]: The lanthanide complexes were prepared by adding an aqueous solution (ca. 20 mL) of the lanthanide salt Ln(NO$_3$)$_3$·5H$_2$O (Ln = Sm^{3+}, Tb^{3+}; 0.889 g, 2.00 mmol and 0.872 g, 2.00 mmol, respectively) to an aqueous solution (ca. 40 mL, pH = 3.0±0.1) containing 2,6-dihydroxybenzoic acid (1.23 g, 8.00 mmol) and KOH (0.448 g, 8.00 mmol). After stirring the mixture for 1 h, an aqueous solution (5 mL) containing tetrabutylammonium chloride hydrate (*n*Bu$_4$NCl·*n*H$_2$O, 1.11 g, 4.00 mmol) was added and a flocculant white solid was immediately formed. The supernant solution was decanted and the precipitate collected and washed with distilled water. Crystals of [*n*Bu$_4$N]$_2$[Ln(2,6-dhb)$_5$(H$_2$O)$_2$] [Ln = Sm^{3+} (**1**) and Tb^{3+} (**2**), respectively], suitable for single-crystal X-ray diffraction were obtained from the filtrate after 1 d.

Preparation of [*n*Bu$_4$N][2,6-dhb]: The 2,6-dhb$^-$ tetrabutylammonium salt, [*n*Bu$_4$N][2,6-dhb], was prepared by adding an aqueous solution (ca. 5 mL) of *n*Bu$_4$NCl·*n*H$_2$O (0.556 g, 2.00 mmol) to an aqueous solution (ca. 10 mL) containing 2,6-dihydroxybenzoic acid (0.308 g, 2.00 mmol) and KOH (0.112 g, 2.00 mmol). After stirring the mixture for 1 h, the white precipitate formed was filtered and washed with distilled water.

Characterisation: IR spectra were measured using KBr disks with a Mattson 7000 FT instrument. Raman spectra were recorded using a Bruker RFS100/S FT-Raman spectrometer (Nd:YAG laser, 1064 nm excitation). ^{1}H spectra were obtained using a Bruker AMX-300 spectrometer (^{1}H, 300 MHz; ^{13}C, 75.4 MHz) referenced to Si(CH$_3$)$_4$ or the solvent. Elemental analyses for carbon, nitrogen and hydrogen were performed with an Exeter Analytical CE-440 Elemental Analyser. The sample was combusted under oxygen at 975 °C for 1 min, with He as the purge gas. The lanthanide content in the complexes was measured by ICP (Analytical Laboratories, University of Aveiro). Powder X-ray diffraction patterns (PXRD) were recorded at ambient temperature using a Philips X'Pert instrument, operating with a monochromated Cu-K_α radiation source at 40 kV/50 mA. Data were collected using the step-counting method (step 0.01°, 7 s per step) in the $2° \leq 2\theta \leq 60°$ range. Theoretical PXRD calculations were performed using the STOE Win XPOW software package.[20] Photoluminescence (PL) spectra, measured between 10 K and room temp. were recorded using a Jobin Yvon-Spex spectrometer (HR, 460) coupled to an R928 Hamamatsu photomultiplier. An Xe arc lamp (150 mW) coupled to a Jobin Yvon monochromator (TRIAX 180) was used as the excitation source. All the spectra were corrected for the response of the detector. The lifetime measurements were carried out using a pulsed Xe arc lamp (5 mJ/pulse, 3 μs bandwidth) coupled to a Kratos GM-252 monochromator and a Spex 1934 C phosphorimeter. The room-temp. triboluminescence (TL) spectra were recorded with a plug-in high-sensitivity fibreoptic UV/Vis shortwave master spectrometer, fitted with a grating blazed at 500 nm with 600 grooves per mm, with a 2048-element linear CCD-array detector (PC, 2000, Ocean Optics, Inc.). A PC 2000 was mounted on a 1 MHz ISA-bus A/D card fitted directly into a desktop PC. The single-crystals of **2** were ground by hand using the plug-in high sensitivity fibre optic.

X-ray Crystallographic Studies: Suitable single crystals of **1** and **2** were mounted on glass fibres using perfluoropolyether oil.[21] Data were collected with a Nonius Kappa CCD diffractometer with Mo-K_α graphite-monochromated radiation (λ = 0.7107 Å). The structures were solved by direct methods and refined by full-matrix least squares on F^2 with anisotropic displacement parameters for all non-hydrogen atoms.[22,23] Multi-scan absorption corrections were also applied.[24] All hydrogen atoms were placed in calculated positions, and refined using a riding model with an isotropic displacement parameter fixed at x times U_{eq} for the atom to which they are bound (x = 1.5 for all the O−H and −CH$_3$ groups, and x = 1.2 for the remaining hydrogen atoms). Bond-length restraints were not applied, except for H atoms associated with the water molecules, for which the O−H and H−O−H distances were restrained to ensure a chemically reasonable geometry for the water molecule. Information concerning crystallographic data collection and structure refinement for **1** and **2** is summarised in Table 1, while selected bond lengths and angles are given in Tables 2 and 3, respectively. CCDC-201808 and -201809 contain supplementary crystallographic data for this paper. These data can be obtained free of charge at www.ccdc.cam.ac.uk/conts/retrieving.html [or from the Cambridge Crystallographic Data Centre,12 Union Road, Cambridge CB2 2EZ, U.K.; Fax: (internat.) + 44-1223/336033; E-mail: deposit@ccdc.cam.ac.uk)].

Acknowledgments

We are grateful to J. Soares for assistance in the triboluminescence measurements, to the University of Aveiro for a PhD research grant (P. C. R. S. S.), and to Fundação para a Ciência e a Tecnologia (Portugal), for financial support through the SFRH/BD/3024/2000 (F. A. A. P.) and SFRH/BPD/11480/2002 (R. A. S. F.), PhD and post-doc scholarships, respectively. We are also grateful for additional financial support from the FCT (grant contract: POCTI/35378/QUI/2000 and POCTI/33653/CTM/2000) supported by FEDER.

[1] N. Arnaud, E. Vaquer, J. Georges, *Analyst* **1998**, *123*, 261−265.
[2] G. F. Sá, O. L. Malta, C. M. Donegá, A. M. Simas, R. L. Longo, P. A. Santa-Cruz, E. F. Silva, Jr., *Coord. Chem. Rev.* **2000**, *196*, 165−195.
[3] G. Vicentini, L. B. Zinner, J. Zukerman-Schpector, K. Zinner, *Coord. Chem. Rev.* **2000**, *196*, 353−382.
[4] J. M. Lehn, *Angew. Chem. Int. Ed. Engl.* **1990**, *29*, 1304−1319.
[5] P. C. R. Soares-Santos, H. I. S. Nogueira, V. Félix, M. G. B. Drew, R. A. Sá Ferreira, L. D. Carlos, T. Trindade, *Chem. Mater.* **2003**, *15*, 100−108.
[6] S. F. M. Ali, V. R. Rao, *J. Inorg. Nucl. Chem.* **1975**, *37*, 1041−1042.
[7] W. Brzyska, Z. Rzaczyńska, A. Kula, M. Jaroniec, *Pol. J. Chem.* **1998**, *72*, 2087−2092.
[8] W. Brzyska, A. Kula, Z. Rzaczyńska, M. Jaroniec, *Pol. J. Chem.* **1998**, *72*, 2524−2530.
[9] T. Glowiak, W. Brzyska, A. Kula, Z. Rzaczyńska, M. Jaroniec, *J. Coord. Chem.* **1999**, *48*, 477−486.
[10] W. P. Griffith, H. I. S. Nogueira, B. C. Parkin, R. N. Sheppard, A. J. P. White, D. J. Williams, *J. Chem. Soc., Dalton Trans.* **1995**, 1775−1781.
[11] G. Bandoli, A. Dolmella, T. I. A. Gerber, J. Perils, J. G. H. Preez, *Inorg. Chim. Acta* **1999**, *294*, 114−118.
[12] F. Cariati, L. Erre, G. Micera, A. Panzanelli, *Inorg. Chim. Acta* **1983**, *80*, 57−65.
[13] G. Smith, C. H. L. Kennard, T. C. W. Mak, *Z. Kristallogr.* **1988**, *184*, 275−280.
[14] T. Glowiack, H. Kozlowski, L. S. Erre, G. Micera, B. Gulinati, *Inorg. Chim. Acta* **1992**, *202*, 43−48.

[15] See, for example: G. A. van Albada, S. Gorter, J. Reedijk, *Polyhedron* **1999**, *18*, 1821; W. Lu, Y. Cheng, N. Dong, C. Xu, C. Chen, *Acta Crystallogr. Sect. C* **1995**, *51*, 1756; J.-G. Mao, H.-J. Zhang, J.-Z. Ni, S.-B. Wang, T. C. W. Mak, *Polyhedron* **1999**, *18*, 1519; J.-F. Ma, Z.-S. Jin, J.-Z. Ni, *Acta Crystallogr. Sect. C* **1994**, *50*, 1008.
[16] C. Oldham, in *Comprehensive Coordination Chemistry*, 1st ed. (Ed.: S. G. Wilkinson), Pergamon Press, Oxford, **1987**, vol. 2, p. 435−459.
[17] M. D. Faucher, R. Morlotti, O. K. Moune, *J. Lumin.* **2002**, *96*, 37−49.
[18] X. Chen, X. Zhu, Y. Xu, S. S. S. Raj, S. Öztürk, H. Fun, J. Ma, X. You, *J. Mater. Chem.* **1999**, *9*, 2919−2922.
[19] A. L. Rheingold, W. King, *Inorg. Chem.* **1989**, *28*, 1715−1719.
[20] STOE, Cie GmbH, *Win XPOW THEO*, Version 1.15, **1999**.
[21] T. Kottke, D. Stalke, *J. Appl. Crystallogr.* **1993**, *26*, 615.
[22] G. M. Sheldrick, *SHELXL 97, Program for Crystal Structure Refinement*, University of Göttingen, **1997**.
[23] G. M. Sheldrick, *SHELXS 97, Program for Crystal Structure Solution*, University of Göttingen, **1997**.
[24] R. H. Blessing, *Acta Crystallogr., Sect. A* **1995**, *51*, 33.

Received February 12, 2003
Early View Article
Published Online August 14, 2003

